5-2018

On the hyperbolicity of the two-fluid model for gas–liquid bubbly flows

Nithin Panicker
Iowa State University

Alberto Passalacqua
Iowa State University, albertop@iastate.edu

Rodney O. Fox
Iowa State University, rofox@iastate.edu

On the hyperbolicity of the two-fluid model for gas–liquid bubbly flows

Abstract
The hyperbolicity condition of the system of partial differential equations (PDEs) of the incompressible two-fluid model, applied to gas–liquid flows, is investigated. It is shown that the addition of a dispersion term, which depends on the drag coefficient and the gradient of the gas volume fraction, ensures the hyperbolicity of the PDEs, and prevents the nonphysical onset of instabilities in the predicted multiphase flows upon grid refinement. A constraint to be satisfied by the coefficient of the dispersion term to ensure hyperbolicity is obtained. The effect of the dispersion term on the numerical solution and on its grid convergence is then illustrated with numerical experiments in a one-dimensional shock tube, in a column with a falling fluid, and in a two-dimensional bubble column.

Keywords
Two-fluid model, Hyperbolicity, Bubbly flows, Bubble dispersion, Shock tube, Bubble column

Disciplines
Analytical Chemistry | Complex Fluids

Comments
This is a manuscript of an article published as Panicker, N., A. Passalacqua, and R. O. Fox. "On the hyperbolicity of the two-fluid model for gas–liquid bubbly flows." *Applied Mathematical Modelling* (2018). DOI: 10.1016/j.apm.2018.01.011. Posted with permission.

On the hyperbolicity of the two-fluid model for gas–liquid bubbly flows

N. Panicker[a], A. Passalacqua[a,*], R. O. Fox[b]

[a] *Department of Mechanical Engineering, Iowa State University, Black Engineering Building, Ames, IA 50011, USA*
[b] *Department of Chemical and Biological Engineering, Iowa State University, Sweeney Hall, Ames, IA, 50011-2230, USA*

Abstract

The hyperbolicity condition of the system of partial differential equations (PDEs) of the incompressible two-fluid model, applied to gas–liquid flows, is investigated. It is shown that the addition of a dispersion term, which depends on the drag coefficient and the gradient of the gas volume fraction, ensures the hyperbolicity of the PDEs, and prevents the nonphysical onset of instabilities in the predicted multiphase flows upon grid refinement. A constraint to be satisfied by the coefficient of the dispersion term to ensure hyperbolicity is obtained. The effect of the dispersion term on the numerical solution and on its grid convergence is then illustrated with numerical experiments in a one-dimensional shock tube, in a column with a falling fluid, and in a two-dimensional bubble column.

Keywords: two-fluid model, hyperbolicity, bubbly flows, bubble dispersion, shock tube, bubble column

1. Introduction

The two-fluid model [1–5] probably represents the most widely adopted approach to describe the spatial and temporal evolution of gas–liquid flows in systems of practical relevance, due to its moderate computational cost. For this reason, the correct formulation of the model has been subject of several studies, which aimed, on one hand, to ensure the desired mathematical

*Corresponding author
Email address: albertop@iastate.edu (A. Passalacqua)

property of hyperbolicity of the model equations, and, on the other hand, to appropriately incorporate the description of physical phenomena experimentally observed in bubbly flows. In particular, the numerical stability of the solution obtained from the two-fluid model depends on the characteristics of the underlying equations, which, as shown in [6–8], may be complex. In such a case, the discretized equations do not allow a grid-converged solution to be achieved, and unstable modes in the solution appear, severely affecting the model prediction and its sensitivity to grid refinement. Several approaches were suggested in the literature to address this problem. Stuhmiller [6] observed that the addition of a certain amount of dissipation mitigates the problem for a specific grid resolution. The problem of complex characteristics was addressed in [9] with the introduction of surface tension effects. A criterion for the grid resolution that ensures the well-posedness of two-fluid problem, relating the minimum grid size to a multiple of the bubble radius, was proposed in [8].

It was demonstrated in [10] that real characteristics of the two-fluid equations are a necessary condition in order not to violate the causality requirement. In particular, his work shows that, when the two-fluid equations have complex characteristics, it is necessary to know all the values at the solution at future times $t > t_i$, in order to determine an accurate solution at an arbitrary time t_i. Such a result clearly violates the physical constraint of causality, and highlights the importance of ensuring that the mathematical model is hyperbolic. Based on these observations, several researchers proposed modified version of the two-fluid model that guarantee hyperbolicity under certain conditions. Some authors [11–13] performed numerical regularization of the ill-posed equation, which, however, comes at the expense of accuracy, since it relies on the addition of numerical dissipation.

Several investigators [6, 9, 14–19] ensured the hyperbolicity of the two-fluid model by introducing a pressure term in the phase momentum equation. The presence of the same mean bulk pressure P_k in both the phases was assumed in [6], and added an interface pressure term $(p_{\mathrm{ki}} - P_{\mathrm{k}})\,\nabla\alpha$, where p_{ki} is the interface pressure for phase k, in order to make the two-fluid model hyperbolic. He considered the interface pressures p_{ki} for both the phases to be equal, and modeled them based on the analytical solution of pressure distribution around an isolated sphere [20]. An interface pressure term $p_{\mathrm{i}}\nabla\alpha$ was used in [14], where, differently from [6], p_i is a coefficient determined to ensure the hyperbolicity of the set of equations, without physical justification. The addition of this term, however, was deemed controversial [12], as shown

by [21].
A study of wave propagation in adiabatic mono-disperse bubbly flows was performed in [22], who concluded that the interfacial pressure difference and the gradients of the void fraction in the non-drag momentum exchange terms dominate the behavior of void wave propagation in bubbly flows.
Real characteristics for the two-fluid model equations were ensured by assuming the mean bulk pressures in both the phases to be different in [9]. These pressures were related through the Laplace constraint, and their difference is set to be proportional to the surface tension. In other works [15–19], the two-fluid model is made hyperbolic using a two-pressure formulation for compressible two-phase flows, where pressures in each phases are computed using an equation of state. However, these authors follow different approaches to model the interface pressure term $(p_{\mathrm{ki}} - P_{\mathrm{k}})\,\nabla\alpha$. The interface pressures p_{ki} were assumed to be equal in [15, 16]. Their model is valid only for stratified flows, and it requires an additional transport equation for the volume fraction in terms of the interface velocity to close the set of equations. Similarly, equal interface pressures were considered in [17], and calculated as a function of the mixture pressure. The interface pressure coefficient $(p_{\mathrm{ki}} - P_{\mathrm{k}})$ was modeled in both the phases in terms of the surface tension and bulk modulus by [17, 23, 24].
Wave propagation analysis in bubbly flows was performed in [25, 26], where it was found the virtual mass term has a significant effect on the dispersion of waves in these flows. The existence of complex characteristics in the two-fluid model with virtual mass term was confirmed by [19, 27]. These authors proposed the introduction of an interfacial pressure jump term, directly proportional to the surface tension between the phases, in order to ensure the hyperbolic behavior of the two-fluid model. The resulting model with virtual mass and interfacial pressure jump was hyperbolic, but the wave dispersion may become excessive, depending on the value of the coefficient used in the virtual mass model. A detailed study of the pressure forces in disperse two-phase flows can be found in [28]. The stability of a two-fluid model containing only first-order differential terms and algebraic closures was studied in [29], showing that the stability properties of the model do not depend on the wavelength of the perturbation, which is unphysical. The study was extended in [28] to incorporate the effect of terms with derivatives of arbitrary order. However, the authors of this study concluded that the introduction of these terms is ineffective at improving the long-wavelength stability of the hyperbolic two-fluid model containing only first-order differential terms.

The stability of a uniform suspension of bubbles was examined in [30], identifying a critical value of volume fraction below which the suspension is stable. This result is confirmed experimentally in [31], where experiments of air injection in bubble columns were performed. The standard two-fluid model, however, predicts flow instabilities also in these conditions, showing an unphysical behavior.

The interfacial momentum transfer term in the two-fluid model was described including a dispersion term proportional to the drag coefficient and to the gradient of the gas volume fraction in [32], where an interfacial pressure jump based on the work of [6, 33] was used. The dispersion coefficient was defined in [32] as a function of the turbulent eddy viscosity. The hyperbolicity of the two-fluid equations was ensured in [12] by modifying the virtual mass coefficient as a function of the volume fraction and of the density ratio of the phases, obtained assuming the multiphase mixture is incompressible. Hyperbolicity and stability of the two-fluid model were studied in [34] in terms of the momentum flux parameters they introduced in the model to incorporate the effect of void fraction and phase velocities. The hyperbolicity condition was then determined to identify when the model equation are *stable*, in a mathematical sense, for specific flow conditions.

The hyperbolicity of a two-fluid model for gas–particle flows was investigated in [35], where a modification of the form of the buoyant term to incorporate the effect of the relative motions of the phases, leading to hyperbolic equations. This development was based on the observation made in [36], where the origin of the complex characteristics of the two-fluid equations was attributed to the buoyancy term. However, for gas–particle systems the compressible particle phase has a separate pressure, function of the granular temperature and of the frictional pressure, which is often sufficient to ensure the conditional hyperbolicity of the two-fluid model for an interval of volume fractions [35, 37].

Lhuillier et al. [38] investigated the well-posedness of the six-equation two-fluid model for dispersed mixtures, with the ultimate goal of obtaining a hyperbolic form of the model. They showed that the two-fluid model with equal pressures satisfies the energy conservation constraint for the mixture. They found that the model for the interfacial pressure proposed by [6] does not respect this constraint, and, consequently is not physical. However, they observed the importance of adding a force term proportional to the gradient of the disperse phase fraction, but opposite in sign, to obtain a hyperbolic set of two-fluid equations. In the same study [38], it was argued that the

combined effects of pseudo-turbulence and added mass may be a way to recover hyperbolic equations.

More recently [39] tried to define a criterion for the grid resolution to avoid the numerical difficulties. Their study, however, did not account for the required momentum exchange terms to properly describe bubbly flows, and did not study the hyperbolicity of the model equations. It is worth observing at this point that approaches that define a minimum grid resolution to ensure that a solution of the model can be obtained do not address the actual challenge of formulating a model that allows a grid-converged solution to be achieved. The constraint on the grid resolution, on one hand, relates a purely numerical aspect of solution procedure to a physical parameter, typically the bubble radius, which has been removed from the equations by means of the averaging procedure. On the other hand, it introduces an arbitrary limit to the spatial scales that can be resolved. As a consequence, a formulation of the two-fluid model that allows a solution to be achieved on an arbitrarily fine grid should be preferred.

Finally, the two-fluid model was made unconditionally hyperbolic by adding an interfacial pressure difference term, proportional to the square of the relative velocity magnitude, and a collision term in [40]. However, the adopted collisional model was developed in [41] considering hard spheres, which may not properly represent the actual physical phenomena affecting a gas-liquid system.

Vazquez-Gonzalez et al. [42] investigated the thermodynamic consistency of various forms and schemes for the two-fluid model. In particular, they studied the acceptability of using an elliptical model for the convective term in the two-fluid model, in order to prevent the dampening of physical instabilities such as the one of Kelvin-Helmoltz [42]. In order to delay the onset of instabilities in their simulation of the Ransom's test with mesh refinement, they relied on a term accounting for a drag force proportional to the gradient of the volume fraction of the disperse phase with the form [42]

$$\mathbf{D} = \frac{\alpha_\mathrm{g}\rho_\mathrm{g}\alpha_\mathrm{l}\rho_\mathrm{l}}{\alpha_\mathrm{g}\rho_\mathrm{l} + \alpha_\mathrm{l}\rho_\mathrm{g}}\delta\mathbf{U}_\mathrm{r}^2\nabla\alpha_\mathrm{g}. \tag{1}$$

In their studies [42], they observed that hyperbolicity is ensured for $\delta > 1$, but this is achieved at the cost of a loss of energy conservation. They observed that a value of $\delta = 0.2$ was sufficient to remove undershoots in their Ransom's test cases, even if the two-fluid model is elliptical. However, they observed [42] that the effect only delays the onset of the instability, which is

problematic in several multiphase flow simulations, which are often transient in nature.

In the present work, we investigate the hyperbolicity of the two-fluid equations examining the role of momentum transfer terms in ensuring this condition. We focus our attention on a dispersion term analogous to the one proposed in [32]. Differently from [32], however, we argue that such a dispersion term should be present also when laminar bubbly flows are considered, since it describes the effect on the drag acting on one bubble due to gradients in the volume fraction of the disperse phase. We propose a closure based on the considerations of [30, 43], with a dispersion coefficient determined to ensure the hyperbolic nature of the two-fluid equations. We demonstrate that the introduction of this dispersion term allows the grid convergence of the two-fluid model to be achieved, without introducing a second pressure term, whose physical justification is not always clear, in particular in the case of incompressible phases.

The remainder of this article is organized as follows: in Sec. 2 the equations of the two-fluid model and the constitutive equations used as closure are summarized. In Sec. 3 the hyperbolicity of the one-dimensional form of the model is investigated, and a constraint on the dispersion coefficient to ensure the hyperbolic nature of the equations is determined. Sec. 6 illustrates an application to a one-dimensional shock tube problem, where the role of the dispersion term in preventing unphysical behavior with grid refinement is demonstrated. The effectiveness of the proposed modification is further tested with numerical experiments performed in a column with falling liquid, with progressively finer grid resolutions, as shown in Sec. 7. Finally, an example application to a two-dimensional bubble column is illustrated in Sec. 8, showing how the addition of the dispersion term removes nonphysical oscillations in the flow, without compromising the experimentally observed fluctuations of the gas plume, which are due to buoyancy.

2. Equations of the two-fluid model for bubbly flows

The equations of the two-fluid model typically used to describe the evolution of gas–liquid systems [1, 3, 4] are summarized in this section, since they are the base of the study discussed in this work, and they are used to perform the numerical experiments here described.

The continuity equation for the generic phase φ is

$$\frac{\partial}{\partial t}\left(\alpha_\varphi \rho_\varphi\right) + \nabla \cdot \left(\alpha_\varphi \rho_\varphi \mathbf{U}_\varphi\right) = 0, \tag{2}$$

where α_φ is the phase fraction, ρ_φ is the thermodynamic density of the phase, and $\mathbf{U}_\varphi$ is the phase velocity.
The phase momentum equation for the liquid phase is

$$\frac{\partial}{\partial t}\left(\alpha_\mathrm{l} \rho_\mathrm{l} \mathbf{U}_\mathrm{l}\right) + \nabla \cdot \left(\alpha_\mathrm{l} \rho_\mathrm{l} \mathbf{U}_\mathrm{l} \otimes \mathbf{U}_\mathrm{l}\right) = \nabla \cdot \boldsymbol{\tau}_\mathrm{l} - \alpha_\mathrm{l} \nabla p + \alpha_\mathrm{l} \rho_\mathrm{l} \mathbf{g} + \mathbf{M}_\mathrm{gl}, \tag{3}$$

while for the gas phase

$$\frac{\partial}{\partial t}\left(\alpha_\mathrm{g} \rho_\mathrm{g} \mathbf{U}_\mathrm{g}\right) + \nabla \cdot \left(\alpha_\mathrm{g} \rho_\mathrm{g} \mathbf{U}_\mathrm{g} \otimes \mathbf{U}_\mathrm{g}\right) = \nabla \cdot \boldsymbol{\tau}_\mathrm{g} - \alpha_\mathrm{g} \nabla p + \alpha_\mathrm{g} \rho_\mathrm{g} \mathbf{g} + \mathbf{M}_\mathrm{lg}, \tag{4}$$

where $\boldsymbol{\tau}_\varphi$ is the phase stress tensor, p is the shared pressure, $\mathbf{g}$ the gravitational acceleration vector, $\mathbf{M}_\mathrm{gl} = -\mathbf{M}_\mathrm{lg}$ is the momentum exchange term, except for buoyancy which is included in the shared pressure. This last term is computed as the sum of the drag $\mathbf{M}_\mathrm{D}$, lift $\mathbf{M}_\mathrm{L}$, virtual mass $\mathbf{M}_\mathrm{VM}$, wall-lubrication $\mathbf{M}_\mathrm{WL}$, and dispersion forces $\mathbf{M}_\mathrm{dis}$. For the purpose of this work, we focus our attention on the drag, virtual mass and dispersion terms because they will be subject of the hyperbolicity study in Sec. 3. We should note that the closure for the phase stress tensor introduces second-order spatial derivatives, which, however, do not lead to the appearance of imaginary characteristics. Thus, in Sec. 3 the tensors $\boldsymbol{\tau}_\varphi$ are set to zero. Stress tensors are, however, preserved in the numerical implementation, and a Newtonian behavior is assumed for each of the phases.
The drag term is defined as $\mathbf{M}_\mathrm{D} = K\mathbf{U}_\mathrm{r}$, where $K = \alpha_\mathrm{g}\rho_\mathrm{l}\beta$, $\mathbf{U}_\mathrm{r}$ is the slip velocity, and

$$\beta = \frac{3}{4}\frac{|\mathbf{U}_\mathrm{r}|}{\mathrm{d}_\mathrm{p}} C_\mathrm{s}, \tag{5}$$

with C_s the drag coefficient, and d_p the bubble diameter.. The virtual mass term is defined, following [44], as

$$\mathbf{M}_\mathrm{VM} = C_\mathrm{VM}\alpha_\mathrm{g}\rho_\mathrm{l}\left(\frac{\mathrm{D}\mathbf{U}_\mathrm{l}}{\mathrm{D}t} - \frac{\mathrm{D}\mathbf{U}_\mathrm{g}}{\mathrm{D}t}\right), \tag{6}$$

where

$$\frac{\mathrm{D}\mathbf{U}_\varphi}{\mathrm{D}t} = \frac{\partial \mathbf{U}_\varphi}{\partial t} + \mathbf{U}_\varphi \cdot \nabla \mathbf{U}_\varphi \tag{7}$$

is the material derivative of the velocity of phase φ. Finally, the bubble dispersion term $\mathbf{M}_{\mathrm{dis}}$ is defined as

$$\mathbf{M}_{\mathrm{dis}} = \frac{\rho_{\mathrm{l}}\beta}{\alpha_{\mathrm{l}}}\delta_{\mathrm{dis}}\nabla\alpha_{\mathrm{g}}, \tag{8}$$

with dispersion coefficient [30, 43]

$$\delta_{\mathrm{dis}} = C_{\mathrm{dis}} d_{\mathrm{p}} |\mathbf{U}_{\mathrm{r}}| \mathrm{H}, \tag{9}$$

$$\mathrm{H} = \sqrt{\alpha_{\mathrm{g}}\alpha_{\mathrm{l}}}, \tag{10}$$

where d_{p} is the diameter of the bubble. The behavior of eigenvalues of the system of PDEs on the choice of function H will be discussed in Sec. 4
Here, C_{dis} is a parameter whose value will be investigated in the next section, and, in our work, is selected to ensure the hyperbolicity of the two-fluid equations. The dispersion term in Eq. (8) is unrelated to the pressure difference between phases but, instead, arises due to the presence of bubble-bubble interactions through the fluid phase.
It was observed in the introduction that some authors [32] used a term formally similar to the one of Eq. (8), but related it to the dispersion of the gas phase caused by turbulent fluctuations. However, it is known [45] that, also in the case of purely laminar flows, the drag force acting on each bubble is affected by the disturbances induced in the liquid-phase velocity field by the other bubbles. This effect is only partially accounted for in two-fluid model simulations, where correlations for the drag force in homogeneous suspensions are typically used, which do not account for the effect of spatial gradients in the volume fraction on the drag force, but only for the presence of other bubbles in homogeneous suspensions [46–49]. The introduction of the dispersion term in Eq. (8) allows the effect of gradients of the volume fraction on the drag force to be taken into account. It is worth noting at this point that the term in Eq. (8) is null in homogeneous suspensions, since the gradient of the gas volume fraction is null, ensuring consistent behavior in the homogeneous limit.
In the next section we will illustrate the role of this dispersion term in ensuring the hyperbolicity of the equations of the two-fluid model, and we determine the dispersion coefficient to ensure the hyperbolic nature of the equations of the two-fluid model.

3. Study of the hyperbolicity of the one-dimensional two-fluid model

We study in this section the hyperbolicity of the set of PDEs describing the evolution of the gas and liquid phase in a gas–liquid system. To this purpose, we consider the one-dimensional two-fluid model, writing its equations in non-conservative form.
The phase continuity equation for the gas phase then reads

$$\frac{\partial \alpha_{\mathrm{g}}}{\partial t} + U_{\mathrm{g}} \frac{\partial \alpha_{\mathrm{g}}}{\partial x} + \alpha_{\mathrm{g}} \frac{\partial U_{\mathrm{g}}}{\partial x} = 0, \tag{11}$$

while, for the liquid phase, it is

$$\frac{\partial \alpha_{\mathrm{l}}}{\partial t} + U_{\mathrm{l}} \frac{\partial \alpha_{\mathrm{l}}}{\partial x} + \alpha_{\mathrm{l}} \frac{\partial U_{\mathrm{l}}}{\partial x} = 0. \tag{12}$$

Similarly, we consider the phase momentum equations in non-conservative form, including the momentum coupling terms due to drag, virtual-mass and dispersion forces. We then have, for the gas phase,

$$\begin{aligned} \alpha_{\mathrm{g}} \left(\rho_{\mathrm{g}} + C_{\mathrm{VM}} \rho_{\mathrm{l}}\right) \frac{\partial U_{\mathrm{g}}}{\partial t} - \alpha_{\mathrm{g}} C_{\mathrm{VM}} \rho_{\mathrm{l}} \frac{\partial U_{\mathrm{l}}}{\partial t} \\ + \frac{\rho_{\mathrm{l}} \beta \delta_{\mathrm{dis}}}{\alpha_{\mathrm{l}}} \frac{\partial \alpha_{\mathrm{g}}}{\partial x} + \alpha_{\mathrm{g}} \frac{\partial p}{\partial x} + \alpha_{\mathrm{g}} U_{\mathrm{g}} \left(\rho_{\mathrm{g}} + C_{\mathrm{VM}} \rho_{\mathrm{l}}\right) \frac{\partial U_{\mathrm{g}}}{\partial x} \\ - \rho_{\mathrm{l}} \alpha_{\mathrm{g}} U_{\mathrm{l}} C_{\mathrm{VM}} \frac{\partial U_{\mathrm{l}}}{\partial x} = -\alpha_{\mathrm{g}} \rho_{\mathrm{l}} \beta \left(U_{\mathrm{g}} - U_{\mathrm{l}}\right) + \alpha_{\mathrm{g}} \rho_{\mathrm{g}} g, \end{aligned} \tag{13}$$

and for the liquid phase

$$\begin{aligned} \rho_{\mathrm{l}} \left(1 - \alpha_{\mathrm{g}} + C_{\mathrm{VM}} \alpha_{\mathrm{g}}\right) \frac{\partial U_{\mathrm{l}}}{\partial t} - \alpha_{\mathrm{g}} C_{\mathrm{VM}} \rho_{\mathrm{l}} \frac{\partial U_{\mathrm{g}}}{\partial t} \\ - \frac{\rho_{\mathrm{l}} \beta \delta_{\mathrm{dis}}}{\alpha_{\mathrm{l}}} \frac{\partial \alpha_{\mathrm{g}}}{\partial x} + \left(1 - \alpha_{\mathrm{g}}\right) \frac{\partial p}{\partial x} - \alpha_{\mathrm{g}} U_{\mathrm{g}} C_{\mathrm{VM}} \rho_{\mathrm{l}} \frac{\partial U_{\mathrm{g}}}{\partial x} \\ + \left[\rho_{\mathrm{l}} \left(1 - \alpha_{\mathrm{g}}\right) U_{\mathrm{l}} + \alpha_{\mathrm{g}} U_{\mathrm{l}} C_{\mathrm{VM}} \rho_{\mathrm{l}}\right] \frac{\partial U_{\mathrm{l}}}{\partial x} \\ = \alpha_{\mathrm{g}} \rho_{\mathrm{l}} \beta \left(U_{\mathrm{g}} - U_{\mathrm{l}}\right) + \left(1 - \alpha_{\mathrm{g}}\right) \rho_{\mathrm{l}} g. \end{aligned} \tag{14}$$

For the purpose of the hyperbolicity study, we rewrite the model equations in matrix form

$$\mathbf{A} \frac{\partial \mathbf{X}}{\partial t} + \mathbf{B} \frac{\partial \mathbf{X}}{\partial x} = \mathbf{C}, \tag{15}$$

where the vector $\mathbf{X}$ is defined as

$$\mathbf{X} = \left[\alpha_{\mathrm{g}}, p, U_{\mathrm{g}}, U_{\mathrm{l}}\right]^{\mathrm{T}}, \tag{16}$$

and the matrices $\mathbf{A}$, $\mathbf{B}$ and $\mathbf{C}$ are

$$\mathbf{A} = \begin{bmatrix} 1 & 0 & 0 & 0 \\ -1 & 0 & 0 & 0 \\ 0 & 0 & \alpha_{\mathrm{g}}\left(\rho_{\mathrm{g}} + C_{\mathrm{VM}}\rho_{\mathrm{l}}\right) & -\alpha_{\mathrm{g}} C_{\mathrm{VM}}\rho_{\mathrm{l}} \\ 0 & 0 & -\alpha_{\mathrm{g}} C_{\mathrm{VM}}\rho_{\mathrm{l}} & \rho_{\mathrm{l}}\left(1 - \alpha_{\mathrm{g}} + \alpha_{\mathrm{g}} C_{\mathrm{VM}}\right) \end{bmatrix}, \tag{17}$$

$$\mathbf{B} = \begin{bmatrix} U_{\mathrm{g}} & 0 & \alpha_{\mathrm{g}} & 0 \\ -U_{\mathrm{l}} & 0 & 0 & 1 - \alpha_{\mathrm{g}} \\ \frac{\rho_{\mathrm{l}}\beta\delta_{\mathrm{dis}}}{\alpha_{\mathrm{l}}} & \alpha_{\mathrm{g}} & \alpha_{\mathrm{g}} U_{\mathrm{g}}\left(\rho_{\mathrm{g}} + C_{\mathrm{VM}}\rho_{\mathrm{l}}\right) & -\rho_{\mathrm{l}}\alpha_{\mathrm{g}} u_{\mathrm{l}} C_{\mathrm{VM}} \\ -\frac{\rho_{\mathrm{l}}\beta\delta_{\mathrm{dis}}}{\alpha_{\mathrm{l}}} & 1 - \alpha_{\mathrm{g}} & -\alpha_{\mathrm{g}} U_{\mathrm{g}} C_{\mathrm{VM}}\rho_{\mathrm{l}} & \rho_{\mathrm{l}}\left(1 - \alpha_{\mathrm{g}}\right) U_{\mathrm{l}} + \alpha_{\mathrm{g}}\rho_{\mathrm{l}} U_{\mathrm{l}} C_{\mathrm{VM}} \end{bmatrix}, \tag{18}$$

and

$$\mathbf{C} = \begin{bmatrix} 0 \\ 0 \\ \alpha_{\mathrm{g}}\rho_{\mathrm{g}} g - \alpha_{\mathrm{g}}\rho_{\mathrm{l}}\beta\left(U_{\mathrm{g}} - U_{\mathrm{l}}\right) \\ \left(1 - \alpha_{\mathrm{g}}\right)\rho_{\mathrm{l}} g + \alpha_{\mathrm{g}}\rho_{\mathrm{l}}\beta\left(U_{\mathrm{g}} - U_{\mathrm{l}}\right) \end{bmatrix}. \tag{19}$$

In order to study the effect of momentum exchange terms on the hyperbolic nature of Eq. (15), we find the characteristic polynomial associated to Eq. (15), defined by

$$|\mathbf{A}\lambda - \mathbf{B}| = 0. \tag{20}$$

The roots of Eq. (20) are real if

$$b^2 - 4ac \geq 0, \tag{21}$$

with

$$a = \alpha_{\mathrm{g}}\left[2\alpha_{\mathrm{g}}\rho_{\mathrm{g}} + \alpha_{\mathrm{g}}^2\rho_{\mathrm{l}} - \left(\rho_{\mathrm{g}} + \rho_{\mathrm{g}}\alpha_{\mathrm{g}}^2 + \rho_{\mathrm{l}}\alpha_{\mathrm{g}} + \rho_{\mathrm{l}} C_{\mathrm{VM}}\right)\right], \tag{22}$$

$$\begin{aligned} b = {} & 2\alpha_{\mathrm{g}}\rho_{\mathrm{g}} U_{\mathrm{g}}\left(1 - 2\alpha_{\mathrm{g}}\right) + 2\alpha_{\mathrm{g}}^2\rho_{\mathrm{l}} U_{\mathrm{l}}\left(1 + C_{\mathrm{VM}}\right) \\ & + 2\alpha_{\mathrm{g}}^3\left(\rho_{\mathrm{g}} U_{\mathrm{g}} - \rho_{\mathrm{l}} U_{\mathrm{l}}\right) + 2C_{\mathrm{VM}}\rho_{\mathrm{l}}\alpha_{\mathrm{g}} U_{\mathrm{g}}\left(1 - \alpha_{\mathrm{g}}\right), \end{aligned} \tag{23}$$

and

$$\begin{aligned} c = {} & \beta\delta_{\mathrm{dis}}\rho_{\mathrm{l}}\alpha_{\mathrm{g}} + \rho_{\mathrm{g}} U_{\mathrm{g}}^2\alpha_{\mathrm{g}}\left(2\alpha_{\mathrm{g}} - 1\right) + \alpha_{\mathrm{g}}^2\rho_{\mathrm{l}} U_{\mathrm{l}}^2\left(\alpha_{\mathrm{g}} - 1\right) \\ & + C_{\mathrm{VM}}\alpha_{\mathrm{g}}^2\rho_{\mathrm{l}}\left(U_{\mathrm{g}}^2 - U_{\mathrm{l}}^2\right) - \alpha_{\mathrm{g}}^3\rho_{\mathrm{g}} U_{\mathrm{g}}^2 - C_{\mathrm{VM}}\alpha_{\mathrm{g}}\rho_{\mathrm{l}} U_{\mathrm{g}}^2. \end{aligned} \tag{24}$$

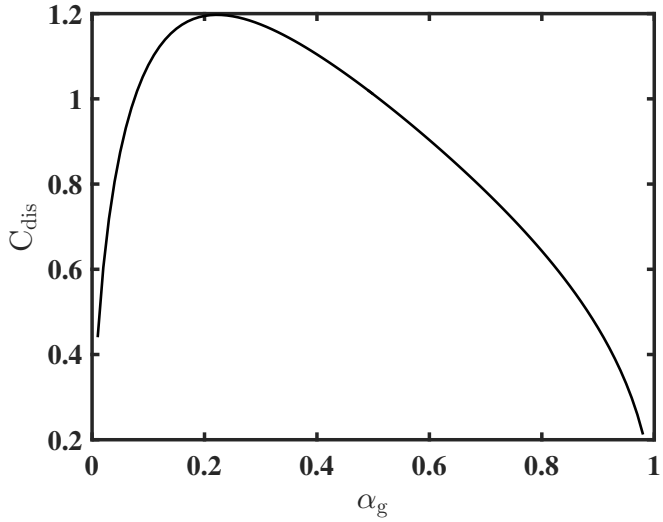

Figure 1: Minimum C_{dis} for large density ratios as a function of gas fraction and $C_{\mathrm{s}} = 0.44$, $C_{\mathrm{VM}} = 0.5$.

The hyperbolicity condition $b^2 - 4ac \geq 0$ leads to the following inequality:

$$\frac{3}{4} C_{\mathrm{s}} C_{\mathrm{dis}} \geq \frac{\sqrt{\alpha_{\mathrm{g}} \left(1 - \alpha_{\mathrm{g}}\right)} \left[\rho_{\mathrm{g}} \left(1 - \alpha_{\mathrm{g}}\right) + \rho_{\mathrm{l}} C_{\mathrm{VM}}\right] \left(1 - \alpha_{\mathrm{g}} + C_{\mathrm{VM}}\right)}{\rho_{\mathrm{l}} \alpha_{\mathrm{g}} \left(1 - \alpha_{\mathrm{g}}\right) + \rho_{\mathrm{g}} \left(1 - \alpha_{\mathrm{g}}\right)^2 + \rho_{\mathrm{l}} C_{\mathrm{VM}}}, \tag{25}$$

where equality identifies the curve of the minimum value of the dispersion coefficient C_{dis} that ensures the system of PDEs in Eq. (15) is hyperbolic.
An example of the hyperbolicity curve for a case with large density ratio ($\rho_{\mathrm{l}} \gg \rho_{\mathrm{g}}$) is shown in Fig. 1, where the virtual mass coefficient is set to $C_{\mathrm{VM}} = 0.5$ [44], and the drag coefficient is set to the constant value $C_{\mathrm{s}} = 0.44$, obtained for a spherical bubble when the Reynolds number based on the slip velocity between the phases is $\mathrm{Re} > 1000$.
The behavior of the curve allows to conclude that, depending on the local value of the gas volume fraction, assuming $\mathrm{Re} > 1000$, the coefficient of the dispersion term in Eq. (9) must be $C_{\mathrm{dis}} \in [0.2, 1.2]$ to ensure that the PDEs that define the two-fluid model are hyperbolic. In particular, in no case can the dispersion term be removed from the phase momentum equations for any value of the gas-phase fractions, if Eq. (15) are desired to be hyperbolic. This is demonstrated in the numerical experiments discussed in the following sections. To conclude the mathematical analysis, we examine a few special

cases that occur when some of the momentum exchange effects are not taken into account:

- If $C_{\mathrm{VM}} = 0$ and $C_{\mathrm{dis}} = 0$, Eq. (20) admits real roots if, and only if, the slip velocity between the phases $U_{\mathrm{g}} - U_{\mathrm{l}}$ is null. This allows us to conclude that the equations of the two-fluid model in Eq. (15) are never hyperbolic if the momentum coupling term only accounts for the drag force without dispersion.

- If $C_{\mathrm{VM}} > 0$ and $C_{\mathrm{dis}} = 0$, Eq. (20) does not admit real roots for any positive value of the virtual mass coefficient C_{VM}. This results implies that Eq. (15) never defines an hyperbolic set of PDEs if the momentum exchange term only incorporates the effect of drag, without dispersion and virtual mass forces.

- The case $C_{\mathrm{VM}} = 0, C_{\mathrm{dis}} > 0$, in which the effect of the virtual mass force is neglected, but the dispersion term is added to the drag force, leads to real roots for Eq. (20) under the condition

$$\frac{3}{4} C_{\mathrm{s}} C_{\mathrm{dis}} \geq \frac{\rho_{\mathrm{g}} \left(1 - \alpha_{\mathrm{g}}\right) \sqrt{\alpha_{\mathrm{g}} \left(1 - \alpha_{\mathrm{g}}\right)}}{\rho_{\mathrm{g}} \left(1 - \alpha_{\mathrm{g}}\right) + \rho_{\mathrm{l}} \alpha_{\mathrm{g}}}, \tag{26}$$

  which is a special case of the proposed regularization in Eq. (25), with $C_{\mathrm{VM}} = 0$.

4. Comparison of eigenvalues with experimental data and determination of H

We obtain the normalized eigenvalues ($\lambda_{\mathrm{i}}/U_{\mathrm{g}}$) of the system of PDEs of the two-fluid model, with the proposed regularization, as a function of α_{g} for flow conditions: $U_{\mathrm{g}} = 0.2m/s$, $C_{\mathrm{dis}} = 1.3$, $\rho_{\mathrm{g}} = 1.2$, and $\rho_{\mathrm{l}} = 1000$ based on a, b and c used in Eq. (22), Eq. (23) and Eq. (24). The eigenvalues computed are compared with the data reported in [50] as shown in Fig. 2(a).
From Fig. 2(a) it can be inferred that the eigenvalues obtained with H = $\sqrt{\alpha_{\mathrm{g}} \left(1 - \alpha_{\mathrm{g}}\right)}$ and $C_{\mathrm{dis}} = 1.3$ are not equal when $\alpha_{\mathrm{g}} \to 0$ and also are not bounded by 1. In reality the eigenvalues, which are otherwise known as the velocity with which the disturbances travel, should be equal for $\alpha_{\mathrm{g}} \to 0$ and always be smaller than the gas velocity U_{g}. This unphysical behavior of the eigenvalues led us to evaluate other coefficients of the proposed

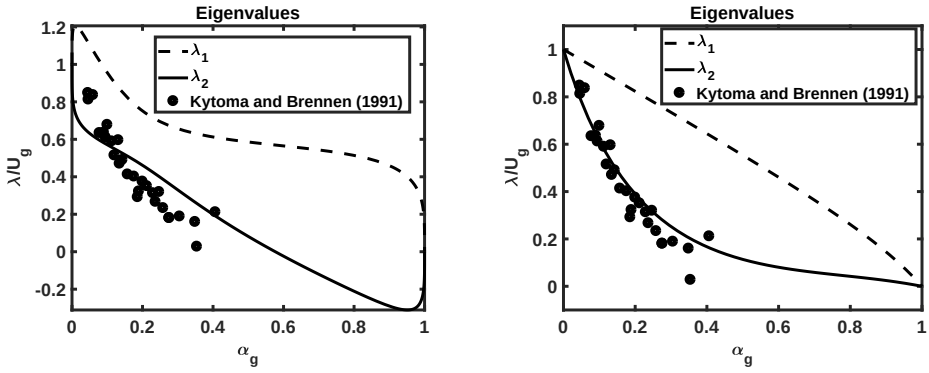

(a) $\mathrm{H} = \sqrt{\alpha_\mathrm{g}\,(1-\alpha_\mathrm{g})}$, $C_\mathrm{dis} = 1.3$. (b) H_{new}, $C_\mathrm{dis} = 4.545$.

Figure 2: Eigen values as a function of α_g for H and H_{new}.

regularization (H functions), which lead to physically realizable eigenvalues. From our study we propose a new form of the H function $\mathrm{H}_{new} = \alpha_\mathrm{g}\,(1-\alpha_\mathrm{g})\left(1 - 1.166\alpha_\mathrm{g} + 0.5\alpha_\mathrm{g}^2\right)$, with a value of the dispersion coefficient $C_\mathrm{dis} = 4.5455$. The proposed H function and C_dis gives realizable eigenvalues which best fit the data of [50] as shown in Fig. 2(b). We highlight here that the choice of the H function is arbitrary, and is semi-empirical in nature. Consequently, other forms are possible which may yield the same results. A physically meaningful expression of Eq. (8) will need to be determined performing, for example, particle-resolved direct numerical simulations on bubble assemblies, in order to determine the effect of gradients in the volume fraction field on the drag force acting on the bubbles.

5. Numerical approach

The two-fluid model was solved using the *reactingTwoPhaseEulerFoam* solver available in the open-source code OpenFOAM [51]. The solver implements a pressure-based solution algorithm designed for a co-located grid arrangement [52]. The checkerboard effect is avoided by means of an improved formulation of the Rhie–Chow interpolation [53, 54]. The buoyancy term is incorporated in the pressure, and other contributions to the momentum exchange term are treated as fluxes, at cell faces [54]. The drag contribution to the momentum exchange term is treated with the partial elimination procedure [55–57]. The boundedness of the phase volume fraction is ensured by a flux-corrected scheme [58]. A second-order scheme with the Sweby [59] limiter is used to re-

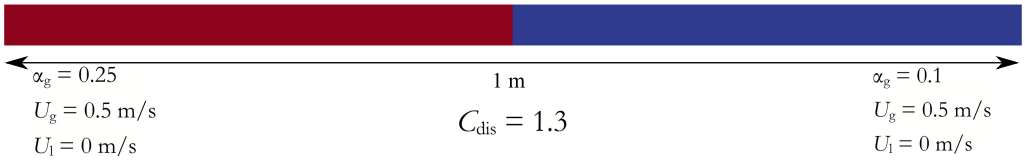

Figure 3: Shock tube geometry and initial conditions.

construct the face value of the flow variables from the corresponding variable at cell centers. A first-order Euler implicit scheme is used for time integration. The time step is adapted to ensure the Courant-–Friedrichs-–Lewy condition is satisfied. Coupling between pressure and velocity is achieved by means of the PIMPLE algorithm [51], which is a combination of the SIMPLE [52, 60] and the PISO procedures [52, 61, 62].

6. One-dimensional two-phase shock tube problem

We consider a one-dimensional shock tube with two incompressible phases to investigate the effect of the dispersion term of Eq. (8) on the numerical solution. We compare the solution of the two-fluid model with and without $\mathbf{M}_{\text{disp}}$ to illustrate that the addition of this term, with a coefficient satisfying the condition of Eq. (25), ensures that the solution of the two-fluid equations consistently converges with grid refinement, without showing non-physical behavior across the discontinuity. The geometry of the shock tube and its configuration are shown in Fig. 3, which also summarizes the initial conditions considered in the numerical experiments. A Neumann boundary condition is specified for all the flow variables U_l, U_g, α_g and p at the left and the right boundaries. The drag coefficient of [63] was used in all the simulations.

As shown in Fig. 4, we consider three progressively finer grid resolutions with 4000, 8000 and 16000 grid cells, respectively, and we compare with the analytical solution.

It is apparent from Fig. 4 that the volume fraction profile along the shock tube predicted by the model without the dispersion term shows a significant undershoot at the location of the discontinuity in the flow properties. Similarly, Fig. 5 shows that, in the absence of the dispersion term, the numerical

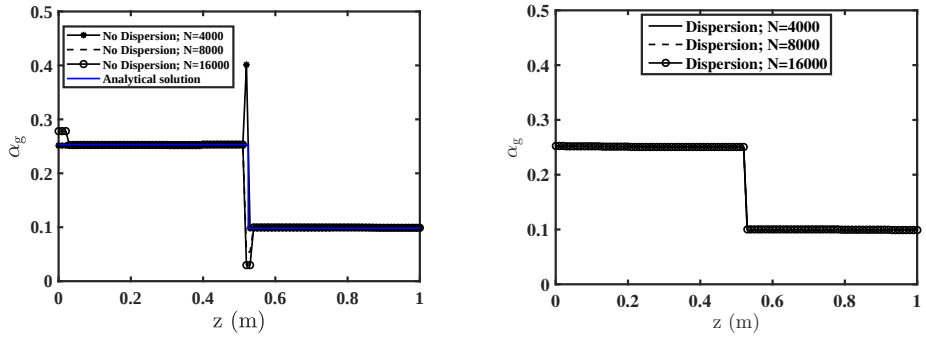

(a) No dispersion. (b) With dispersion.

Figure 4: Volume fraction profiles of the gas phase in the shock tube problem at $t = 0.13$ s.

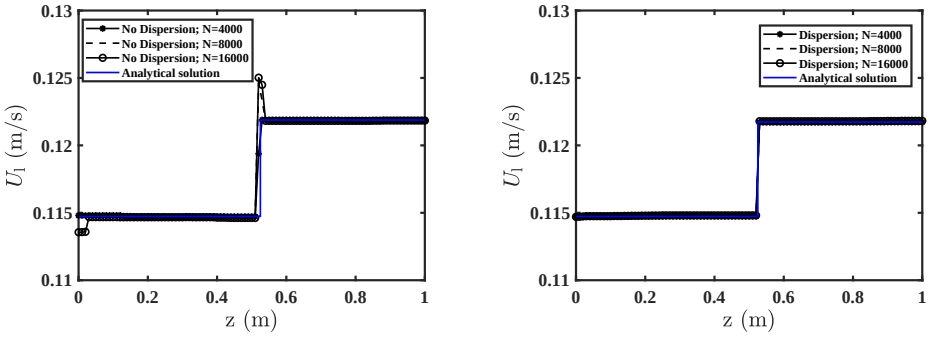

(a) No dispersion. (b) With dispersion.

Figure 5: Liquid velocity profiles of the gas phase in the shock tube problem at $t = 0.13$ s.

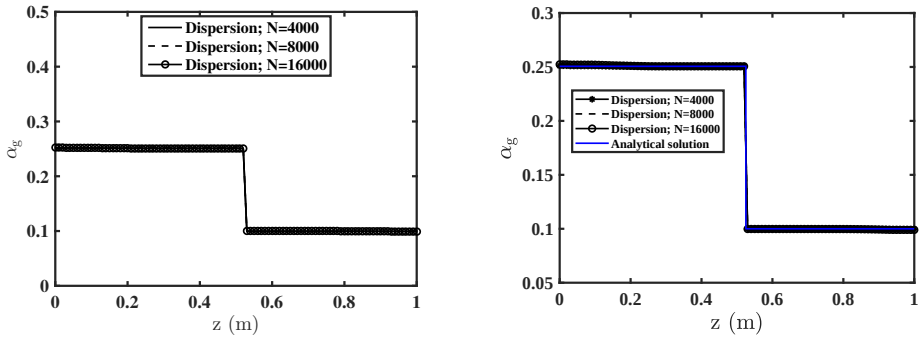

(a) H_{old}. (b) H_{new}.

Figure 6: Volume fraction profiles of the gas phase in the shock tube problem at $t = 0.13$ s for H_{old} and H_{new}.

predictions show overshoots in the liquid velocity. This is clearly incorrect, since the analytical solution is a sharp change in the gas-phase fraction, without overshoot and undershoot. We also note that the problem becomes more serious when the resolution of the computational grid is increased. The solution obtained after the addition of the dispersion term of Eq. (8), on the other hand, does not present the nonphysical behavior of overshoot and undershoot observed when this term is absent. Additionally, in the case with the dispersion term, the numerical solution converges with grid refinement, which numerically demonstrates the grid independence of the solution.
Fig. 6 shows the comparison of volume fraction for H_{old} and H_{new} discussed in sec. 4. The choice of H did not affect the numerical simulation.

7. One-dimensional falling fluid problem

We repeat the numerical experiment of grid refinement described in Sec. 6 in a system constituted by a one-dimensional disperse two-phase system with a region with higher volume fraction of the liquid phase at the top ($\alpha_g = 0.1$), and falling under the effect of gravity into a region with lower liquid volume fraction ($\alpha_g = 0.25$). The geometric configuration and the initial conditions of the problem are reported in Fig. 7. The same closure models used in Sec. 6 are used for all the simulations discussed in this section.
The profiles of volume fraction at $t = 1$ s, with 8,000, 16,000 and 32,000 grid cells, are reported in Fig. 8. The profiles obtained without the dispersion term show nonphysical behavior across the discontinuity in the profile, which

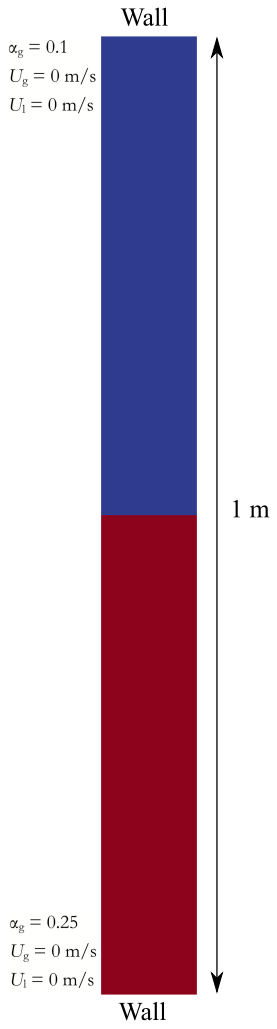

Figure 7: Falling liquid geometry and initial conditions.

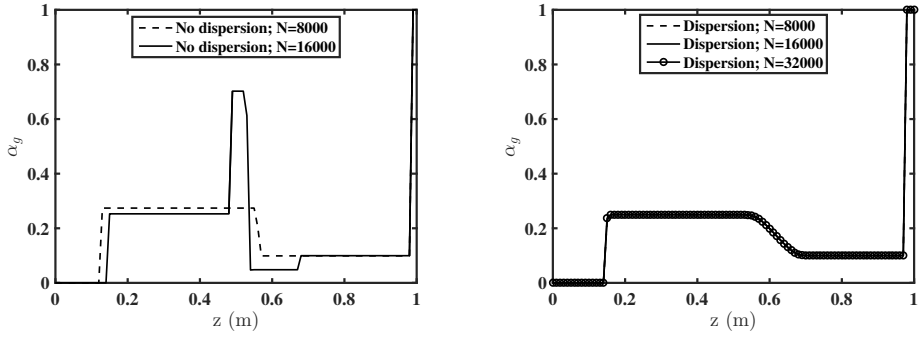

(a) No dispersion. (b) With dispersion.

Figure 8: Volume fraction profiles of the gas phase in the falling fluid problem at $t = 1$ s.

manifest with undershoot and overshoot in the values of the volume fraction. The introduction of the dispersion term addresses the problem, leading to the expected results, and to a convergent solution with grid refinement. The solution for the grid with 32,000 cells without the dispersion term is not reported because the numerical procedure was unable to provide a solution and terminated with an error in such a case (i.e., nonphysical values for α_g). This numerical difficulty disappeared with the introduction of the dispersion term. These observations are reflected also in the velocity profiles of the gas (Fig. 9) and of the liquid (Fig. 10). Fig. 11 shows the comparison of volume fraction for $\mathrm{H_{old}}$ and $\mathrm{H_{new}}$ discussed in Sec. 4. The choice of H did not affect the numerical simulation.

It is worth highlighting that the proposed enforcement of hyperbolicity suppresses the Kelvin-Helmoltz instability, observed in counter-current flows, which appear in the problem under consideration, and becomes particularly evident when pure liquid and gas are present (full phase separation) [64]. In such cases, the behavior introduced by the dispersive term proposed in this work, whose focus is on disperse flows, may be undesired.

8. Application to an example bubble column

A two-dimensional bubble column, 45 cm tall and 10 cm wide, was considered to study the effect of the dispersion term proposed in this work on the prediction of a typical gas–liquid flow encountered in applications. In particular, the solution of the two-fluid model is reported for different grid resolutions (44×200, 88×400, 166×800, 322×1600) to illustrate how

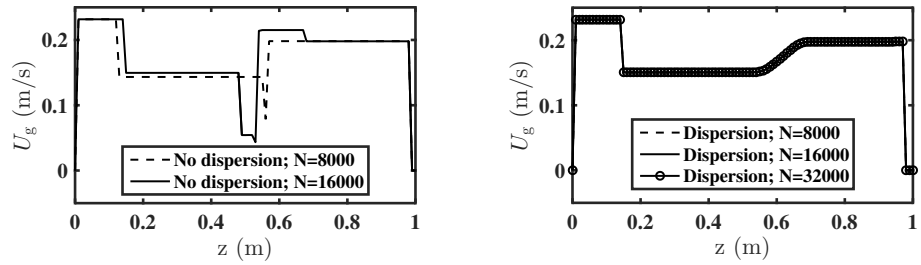

(a) No dispersion. (b) With dispersion.

Figure 9: Gas-phase velocity profiles in the falling fluid problem at $t = 1$ s.

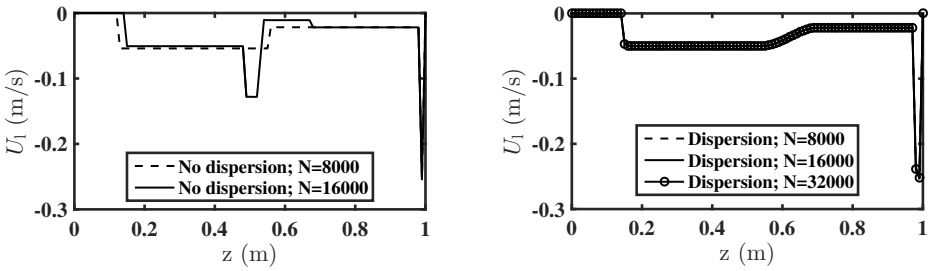

(a) No dispersion. (b) With dispersion.

Figure 10: Liquid-phase velocity profiles in the falling fluid problem at $t = 1$ s.

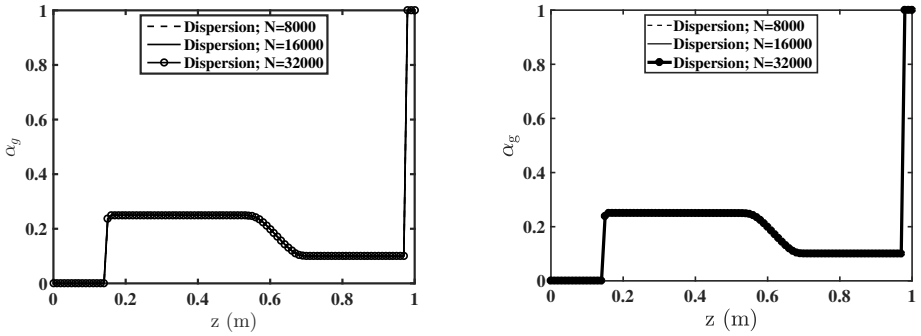

(a) H_{old}. (b) H_{new}.

Figure 11: Volume fraction profiles of the gas phase in the falling fluid problem at $t = 1$ s for H_{old} and H_{new}.

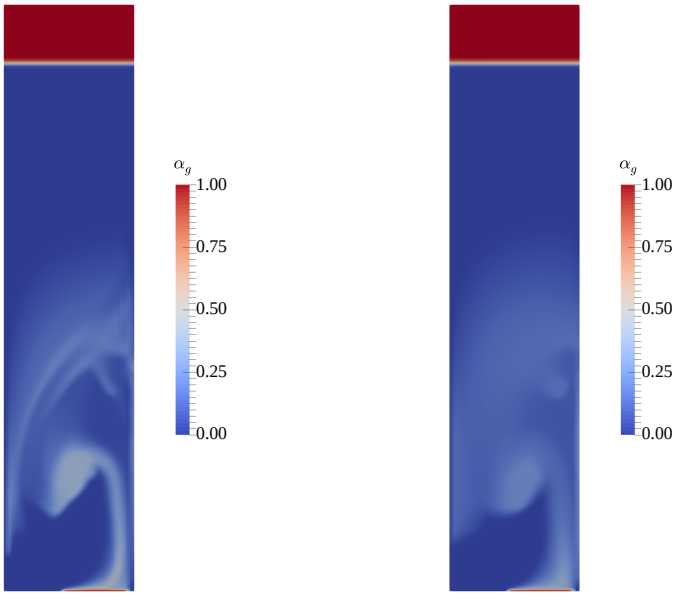

(a) No dispersion (b) With dispersion

Figure 12: Color map of volume fraction in bubble column at $t = 1$ s, with grid resolution of 44×200.

the addition of the dispersion term, on one hand, allows a grid-convergent solution to be reached, and, on the other hand, that the absence of the term leads to the predictions of nonphysical structures with high concentration of gas not observed in experiments.

The drag coefficient in these simulations is modeled following [63], the lift force coefficient was calculated using the expression of [65], and the wall-lubrication force with the model of [66]. The virtual mass coefficient was set to $C_{\mathrm{VM}} = 0.5$ [44].

The bubble column is initially filled with water ($\rho_{\mathrm{l}} = 1000$ kg m^{-3}, $\mu_{\mathrm{l}} = 8.90 \times 10^{-4}$ Pa s) up to the height of 38 cm. Air is injected through an orifice located at the bottom-right of the column, with a velocity whose only non-zero component is vertical, with a magnitude of 5 cm s^{-1}. The orifice is 5 cm wide, and its rightmost side is at a distance of 5 mm from the right wall of the column. The no-slip condition is applied to walls for both the phases, while the pressure is set to the atmospheric at the outlet, located at the top of the column, where a Neumann condition is used for all other variables.

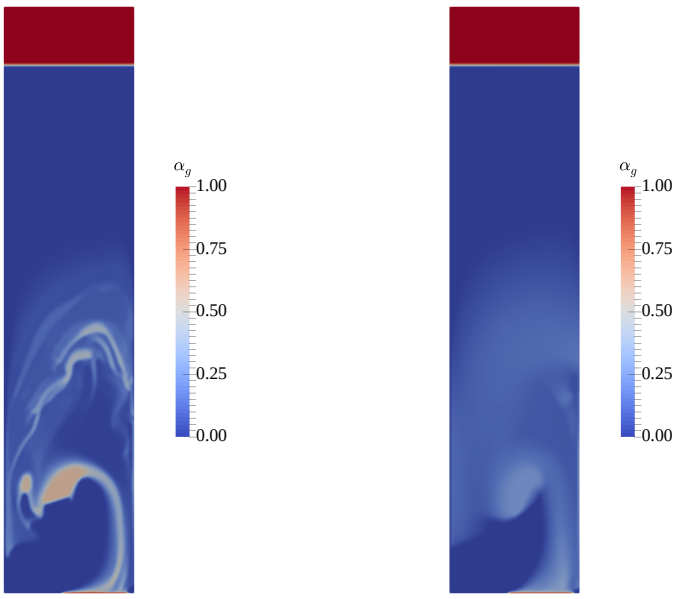

(a) No dispersion (b) With dispersion

Figure 13: Color map of volume fraction in bubble column at $t = 1$ s, with grid resolution of 88×400.

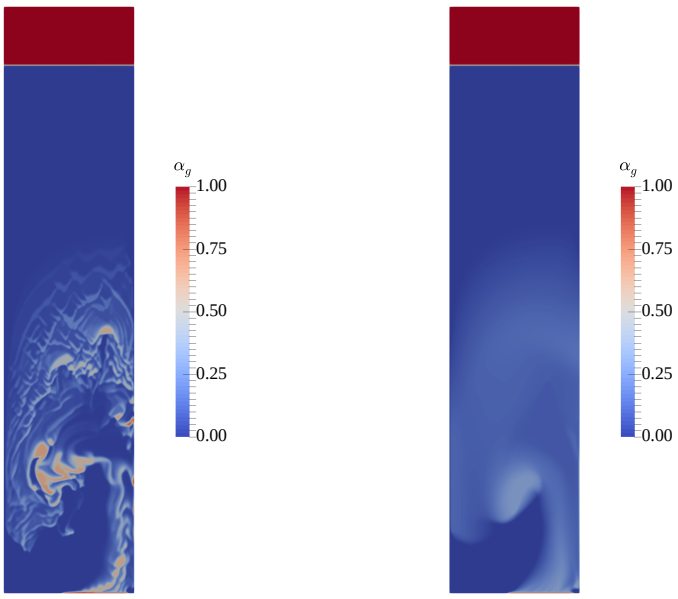

(a) No dispersion (b) With dispersion

Figure 14: Color map of volume fraction in bubble column at $t = 1$ s, with grid resolution of 166×800.

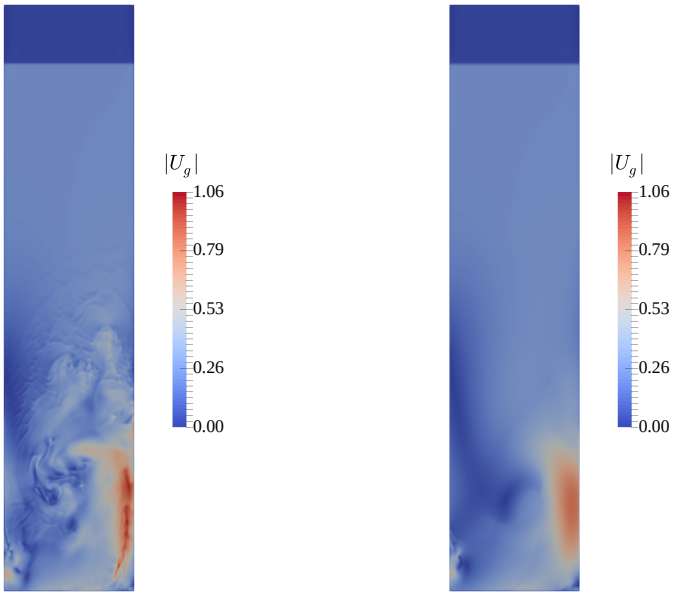

(a) No dispersion (b) With dispersion

Figure 15: Color map of gas velocity in bubble column at $t = 1$ s, with grid resolution of 166×800.

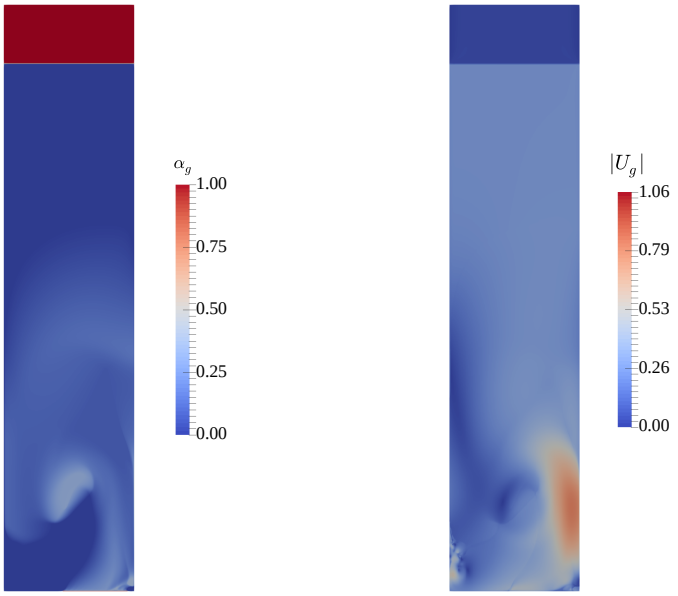

(a) α_g (b) $|U_g|$

Figure 16: Color map of gas volume fraction and of gas velocity in bubble column at $t = 1$ s, with grid resolution of 322×1600 and dispersion term.

Figs. 12, 13 and 14 show the color maps of the gas volume fraction in the bubble column in an instantaneous snapshot taken at $t = 1$ s of actual flow time. It is apparent that, in absence of the dispersion term, the numerical solution shows structures in the flow not observed experimentally, whose size depends on the grid resolution, and in which the value of the gas-phase volume fraction increases with grid refinement. From a numerical perspective, this sensitivity of the model to the grid resolution does not allow a grid-converged solution to be achieved, while, from the perspective of correctly describing the physical flow behavior, it leads to the prediction of features that are not observed in experiments, such as an excess of bubble clustering and a premature onset of flow instability in homogeneous suspension of bubbles. Similar structures are observed in the gas-phase velocity field, as shown in Fig. 15(a), and, consequently, in the liquid velocity field (not reported here). The introduction of the dispersion term described in Sec. 2 addresses the prediction of these nonphysical features by ensuring the hyperbolicity of the model equations, without qualitatively altering the large-scale unsteady behavior of the gas plume, due to buoyancy and the consequent recirculation flow observed in the column.

Observing the sequence of Figs. 12(b), 13(b), 14(b), 15(b), 16(a), we conclude that the addition of the dispersion term also allows a grid-converged solution to be achieved for the fields of gas volume fraction and velocity. The velocity field shows some small structures on the bottom-left of Fig. 15(b) that may be interpreted as oscillations, questioning the stabilizing effect of the dispersion term. However, further grid refinement (Fig. 16) shows that these structures do not become finer with the increased grid resolution, and do not originate oscillations that amplify with grid refinement. This indicates that the finer grid resolution is resolving structures of the flow that were not captured by the coarser grids. Furthermore, these results stress the importance of including the dispersion term in order to achieve the desired level of spatial accuracy. Indeed, when the dispersion term is removed, structures not experimentally observed in bubbly flows are predicted by the two-fluid model.

9. Conclusions

The effect of the momentum transfer term on the hyperbolicity of the equations of the two-fluid model with shared pressure was investigated. It was shown that the introduction of a dispersion term, whose role is to account

for the effects of gradients in the volume fraction on the drag force, leads to a conditionally hyperbolic set of equations depending on the value assigned to the dispersion coefficient. An expression for the minimum value of the dispersion coefficient that ensures the hyperbolic nature of the equations of the two-fluid model was obtained.

The proposed dispersion term was applied to the simulation of two one-dimensional problems, involving a shock tube and a falling liquid. In both cases it was shown that the absence of the dispersion term leads to nonphysical profiles in the flow variables where sharp discontinuities are present. The solution of the model without the dispersion term (non-hyperbolic model) also prevented a grid-converged solution to be achieved. The results obtained with the dispersion term (hyperbolic model) provided the expected results across sharp discontinuities, and led to a numerical solution convergent with grid refinement.

An example of a two-dimensional bubble column was considered to illustrate the role of the hyperbolicity of the equations of the two-fluid model in applications of practical interest. It was observed that, in the absence of the dispersion term, the numerical solution remained sensitive to the grid resolution even at the finest grid refinement used in this work, and showed the presence of nonphysical regions with high concentration of disperse phase, which are not observed experimentally. These artifacts were not observed in the same simulations repeated with the hyperbolic two-fluid model.

Finally, it is worth highlighting that the coefficient obtained here for the dispersion term is based on mathematical considerations, with the purpose of ensuring the hyperbolic behavior of the two-fluid equations. The physically correct formulation of the coefficient, as well as the impact on the agreement of the model predictions with experimental measurements needs further investigation. However, the presence of the dispersion term is needed in both laminar and turbulent flows, in order to account for the effect of gradients of the volume fraction on the drag force. Physically consistent models for the coefficient could be obtained, for example, by performing direct numerical simulations on ensembles of buoyant particles with gradients in the volume fraction.

10. Acknowledgements

The authors gratefully acknowledge support from the US National Science Foundation through grant NSF–CBET1438143. A. P. and N. S. P. wish to

express their gratitude for the support of the American Chemical Society – Petroleum Research Fund through the award PRF # 53924 – DNI9.

References

[1] D. A. Drew, Averaged equations for two-phase flows, Studies in Applied Mathematics L (3) (1971) 205 – 231.

[2] M. Ishii, Thermo-fluid dynamic theory of two-phase flow, Eyrolles, Paris, 1975.

[3] D. A. Drew, Continuum modeling of two-phase flows, in: R. Meyer (Ed.), Theory of Dispersed Multiphase Flow, Academic Press, 1983, pp. 173 – 190.

[4] D. A. Drew, Mathematical modeling of two-phase flow, Annual Review of Fluid Mechanics 15 (1) (1983) 261 – 291.

[5] R. Jackson, Locally averaged equations of motion for a mixture of identical spherical particles and a Newtonian fluid, Chemical Engineering Science 52 (15) (1997) 2457 – 2469.

[6] J. H. Stuhmiller, The influence of interfacial pressure forces on the character of two-phase flow model equations, International Journal of Multiphase Flow 3 (6) (1977) 551 – 560.

[7] R. Lyczkowski, D. Gidaspow, C. Solbrig, E. D. Hughes, Characteristics and stability analyses of transient one-dimensional two-phase flow equations and their finite difference approximations, Nuclear Science and Engineering 66 (3) (1978) 378 – 396.

[8] H. B. Stewart, Stability of two-phase flow calculation using two-fluid models, Journal of Computational Physics 33 (2) (1979) 259 – 270.

[9] J. D. Ramshaw, J. A. Trapp, Characteristics, stability, and short-wavelength phenomena in two-phase flow equation systems, Nuclear Science and Engineering 66 (1) (1978) 93 – 102.

[10] J. P. Sursock, Causality violation of complex-characteristic two-phase flow equations, International Journal of Multiphase Flow 8 (3) (1982) 291 – 295.

[11] A. D. Fitt, The numerical and analytical solution of ill-posed systems of conservation laws, Applied Mathematical Modelling 13 (11) (1989) 618 – 631.

[12] I. Tiselj, S. Petelin, Modelling of two-phase flow with second-order accurate scheme, Journal of Computational Physics 136 (2) (1997) 503 – 521.

[13] T. N. Dinh, R. R. Nourgaliev, T. G. Theofanous, Understanding the ill-posed two-fluid model, in: Proceedings of the 10th International Topical Meeting on Nuclear Reactor Thermal-hydraulics (NURETH03), South Korea, 2003.

[14] D. Bestion, The physical closure laws in the CATHARE code, Nuclear Engineering and Design 124 (3) (1990) 229 – 245.

[15] S. Banerjee, A. Chan, Separated flow models – I. Analysis of the averaged and local instantaneous formulations, International Journal of Multiphase Flow 6 (1 – 2) (1980) 1 – 24.

[16] V. H. Ransom, D. L. Hicks, Hyperbolic two-pressure models for two-phase flow, Journal of Computational Physics 53 (1) (1984) 124 – 151.

[17] R. Saurel, R. Abgrall, A multiphase Godunov method for compressible multifluid and multiphase flows, Journal of Computational Physics 150 (2) (1999) 425 – 467.

[18] S.-J. Lee, K.-S. Chang, S.-J. Kim, Surface tension effect in the two-fluids equation system, International Journal of Heat and Mass Transfer 41 (18) (1998) 2821 – 2826.

[19] M. S. Chung, S. J. Lee, K. S. Chang, Effect of interfacial pressure jump and virtual mass terms on sound wave propagation in the two-phase flow, Journal of Sound and Vibration 244 (4) (2001) 717 – 728.

[20] H. Lamb, Hydrodynamics, Cambridge University Press, 1932.

[21] W. T. Sha, S. L. Soo, On the effect of $p\nabla\alpha$ term in multiphase mechanics, International Journal of Multiphase Flow 5 (2) (1979) 153 – 158.

[22] J. W. Park, D. A. Drew, J. Lahey, R. T., The analysis of void wave propagation in adiabatic monodispersed bubbly two-phase flows using an ensemble-averaged two-fluid model, International Journal of Multiphase Flow 24 (7) (1999) 1205–1244. doi:10.1016/S0301-9322(98)00020-2.

[23] M.-S. Chung, Characteristic development of hyperbolic two-dimensional two-fluid model for gas–liquid flows with surface tension, Applied Mathematical Modelling 31 (3) (2007) 578–588.

[24] Y.-G. Jung, M.-S. Chung, S.-J. Yi, K.-S. Chang, An implementation of the hll scheme on a hyperbolic two-fluid model for two-phase flow simulations, Applied Mathematical Modelling 37 (4) (2013) 2588–2599.

[25] W. Hancox, R. Ferch, W. Liu, R. Nieman, One-dimensional models for transient gas-liquid flows in ducts, International Journal of Multiphase Flow 6 (1) (1980) 25 – 40.

[26] L. Y. Cheng, D. A. Drew, R. T. Lahey, An analysis of wave propagation in bubbly two-component, two-phase flow, Journal of Heat Transfer 107 (2) (1985) 402 – 408.

[27] A. R. D. Thorley, D. C. Wiggert, The effect of virtual mass on the basic equations for unsteady one-dimensional heterogeneous flows, International Journal of Multiphase Flow 11 (2) (1985) 149 – 160.

[28] A. Prosperetti, A. V. Jones, Pressure forces in disperse two-phase flow, International Journal of Multiphase Flow 10 (4) (1984) 425 – 440.

[29] A. V. Jones, A. Prosperetti, On the suitability of first-order differential models for two-phase flow prediction, International Journal of Multiphase Flow 11 (2) (1985) 133 – 148.

[30] A. Biesheuvel, W. C. M. Gorissen, Void fraction disturbances in a uniform bubbly fluid, International Journal of Multiphase Flow 16 (2) (1990) 211 – 231.

[31] W. Harteveld, Bubble Columns: Structure or Stability?, Ph.D. Thesis, Technische Universiteit Delft (2005).

[32] M. R. Davidson, Numerical calculations of two-phase flow in a liquid bath with bottom gas injection: the central plume, Applied Mathematical Modelling 14 (2) (1990) 67 – 76.

[33] C. Pauchon, S. Banerjee, Interphase momentum interaction effects in the averaged multifield model, International Journal of Multiphase Flow 12 (4) (1986) 559 – 573.

[34] J. H. Song, M. Ishii, On the stability of a one-dimensional two-fluid model, Nuclear Engineering and Design 204 (1 –- 3) (2001) 101 – 115.

[35] M. Syamlal, A hyperbolic model for fluid – solids two-phase flow, Chemical Engineering Science 66 (19) (2011) 4421 – 4425.

[36] J. X. Bouillard, R. W. Lyczkowski, S. Folga, D. Gidaspow, G. F. Berry, Hydrodynamics of erosion of heat exchanger tubes in fluidized bed combustors, The Canadian Journal of Chemical Engineering 67 (2) (1989) 218 – 229.

[37] D. Gidaspow, Multiphase Flow and Fluidization, Academic Press, 1994.

[38] D. Lhuillier, C.-H. Chang, T. G. Theofanous, On the quest for a hyperbolic effective-field model of disperse flows, Journal of Fluid Mechanics 731 (2013) 184–194.

[39] R. Picardi, L. Zhao, F. Battaglia, On the ideal grid resolution for two-dimensional eulerian modeling of gas-liquid flows, Journal of Fluids Engineering 138 (11) (2016) 114503–114503.

[40] A. Vaidheeswaran, M. L. de Bertodano, Stability and convergence of computational eulerian two-fluid model for a bubble plume, Chemical Engineering Science 160 (2017) 210–226.

[41] A. Alajbegovic, D. Drew, R. Lahey Jr., An analysis of phase distribution and turbulence in dispersed particle/liquid flows, Chemical Engineering Communications 174 (1999) 85–133, cited By 32.

[42] T. Vazquez-Gonzalez, A. Llor, C. Fochesato, Ransom test results from various two-fluid schemes: Is enforcing hyperbolicity a thermodynamically consistent option?, International Journal of Multiphase Flow 81 (Supplement C) (2016) 104–112.

doi:10.1016/j.ijmultiphaseflow.2015.12.007.
URL http://www.sciencedirect.com/science/article/pii/S0301932215002773

[43] G. K. Batchelor, A new theory of the instability of a uniform fluidized bed, Journal of Fluid Mechanics 193 (1988) 75–110.

[44] D. A. Drew, R. T. Lahey, The virtual mass and lift force on a sphere in rotating inviscid flow, International Journal of Multiphase Flow 13 (1) (1987) 113 – 121.

[45] H. Faxén, Der Widerstand gegen die Bewegung einer starren Kugel in einer zähen Flüssigkeit, die zwischen zwei parallelen ebenen Wänden eingeschlossen ist, Annalen der Physik 373 (10) (1922) 89 – 119.

[46] C. Y. Wen, Y. H. Yu, Mechanics of fluidization, Chem. Eng. Prog. S. Ser. 62 (1966) 100–111.

[47] R. Beetstra, M. A. van der Hoef, J. A. M. Kuipers, A lattice-Boltzmann simulation study of the drag coefficient of clusters of spheres, Computers & Fluids 35 (8–9) (2006) 966–970. doi:10.1016/j.compfluid.2005.03.009.

[48] R. Beetstra, M. A. van der Hoef, J. a. M. Kuipers, Drag force of intermediate Reynolds number flow past mono- and bidisperse arrays of spheres, AIChE Journal 53 (2) (2007) 489–501. doi:10.1002/aic.11065.

[49] S. Tenneti, R. Garg, S. Subramaniam, Drag law for monodisperse gas–solid systems using particle-resolved direct numerical simulation of flow past fixed assemblies of spheres, International Journal of Multiphase Flow 37 (9) (2011) 1072–1092. doi:10.1016/j.ijmultiphaseflow.2011.05.010.

[50] H. Kytömaa, C. Brennen, Small amplitude kinematic wave propagation in two-component media, International journal of multiphase flow 17 (1) (1991) 13–26.

[51] OpenFOAM, OpenFOAM User Guide, The OpenFOAM Foundation, 2016.
URL www.openfoam.org

[52] J. H. Ferziger, M. Peric, Computational Methods for Fluid Dynamics, Springer, 2002.

[53] C. M. Rhie, W. L. Chow, Numerical study of the turbulent flow past an isolated airfoil with trailing edge separation, AIAA Journal 21 (11) (1983) 1525 – 1532.

[54] S. Zhang, X. Zhao, General formulations for Rhie-Chow interpolation, in: 2004 ASME Heat Transfer/Fluids Engineering Summer Conference, no. HT-FED04-56274, Charlotte, North Carolina, USA, 2004, pp. 567 – 573.

[55] D. B. Spalding, Numerical computation of multi-phase fluid flow and heat transfer, in: C. Taylor (Ed.), Recent Advances in Numerical Methods in Fluids, Pineridge Press, 1980.

[56] D. B. Spalding, Developments in the IPSA procedure for numerical computation of multiphase-flow phenomena with interphase slip, unequal temperatures, etc., in: T. M. Shih (Ed.), Numerical Methodologies in Heat Transfer, 1983, pp. 421 – 436.

[57] H. Karema, S. Lo, Efficiency of interphase coupling algorithms in fluidized bed conditions, Computers and Fluids 28 (1999) 323 – 360.

[58] H. G. Weller, Bounded explicit and implicit second-order schemes for scalar transport, Tech. rep., The OpenFOAM Foundation (2006).

[59] P. Sweby, High resolution schemes using flux limiters for hyperbolic conservation laws, SIAM Journal on Numerical Analysis 21 (5) (1984) 995 – 1011.

[60] S. V. Patankar, Numerical Heat Transfer and Fluid Flow, Hemisphere, Washington D. C., 1980.

[61] R. I. Issa, Solution of the implicitly discretised fluid flow equations by operator-splitting, Journal of Computational Physics 62 (1) (1986) 40 – 65.

[62] P. J. Oliveira, R. I. Issa, An improved PISO algorithm for the computation of buoyancy-driven flows, Numerical Heat Transfer, Part B: Fundamentals 40 (6) (2001) 473 – 493.

[63] A. Tomiyama, I. Kataoka, I. Zun, T. Sakaguchi, Drag coefficients of single bubbles under normal and micro gravity conditions, JSME International Journal Series B 41 (2) (1998) 472 – 479.

[64] M. Lopez de Bertodano, W. D. Fullmer, A. Clausse, One-dimensional two-fluid model for wavy flow beyond the Kelvin–Helmholtz instability: Limit cycles and chaos, Nuclear Engineering and Design 310 (Supplement C) (2016) 656–663. doi:10.1016/j.nucengdes.2016.05.038.
URL http://www.sciencedirect.com/science/article/pii/S0029549316301716

[65] D. Legendre, J. Magnaudet, The lift force on a spherical bubble in a viscous linear shear flow, Journal of Fluid Mechanics 368 (1998) 81 – 126.

[66] S. P. Antal, R. T. Lahey Jr., J. E. Flaherty, Analysis of phase distribution in fully developed laminar bubbly two-phase flow, International Journal of Multiphase Flow 17 (5) (1991) 635 – 652.